Bending Models for Thin Flexible Objects

B. Thomaszewski*
WSI/GRIS,
Sand 14, D-72076 Tübingen, Germany,
and
M. Wacker†
HTW university of applied sciences Dresden,
Friedrich-List-Platz 1, 01069 Dresden.

ABSTRACT

Textiles usually exhibit much larger resistance to in-plane deformation than to bending deformation. However, the latter essentially determines the formation of folds and wrinkles which in turn govern the overall appearance of the cloth. The resulting numerical problem is inherently stiff and hence susceptible to instability. This overview is devoted to a closer investigation of bending deformation. Approaches known from the field of engineering can describe the problem of bending in a physically accurate way. However, the nature of the governing equations is such that they cannot be discretised with the standard methods currently used in cloth simulation. Since curvature is a central variable, we introduce related concepts from differential geometry and describe the transition to the discrete setting. Different approaches are discussed and demands on an approach for correctly modelling the bending behaviour of cloth are formulated.

Keywords cloth simulation, physically based simulation, bending

1 Introduction

The most salient characteristic of thin flexible objects is their bending behaviour. Typically, objects from this category show a relatively large resistance to in-plane deformations such as stretching and shearing while the forces due to out-of-plane deformation, i.e. bending, are small. However, this does not mean that the treatment of bending is less important. On the contrary, due to these different reactions to deformation the characteristic folds and wrinkles that we associate with garments are actually formed. Especially in the case of compressive in-plane deformation, i.e. when buckling occurs, the bending behaviour is crucial. Despite its importance, bending has rather been neglected in the physically based simulation of clothes. In contrast, for modelling the in-plane properties of fabrics sophisticated and accurate models are used [BHW94, EWS96]. We think that this discrepancy should be addressed. While this paper provides an introduction to the problem of bending for thin flexible objects, we report on a related implementation and give examples of cloth for illustration in [TWS05].

This overview starts with a look at how existing techniques for cloth simulation deal with bending, including the way curvature is approximated. Subsequently, approaches to bending dominated problems from the field of engineering will be examined more closely. These methods allow a description in a physically accurate way. At the same time however, the governing equations cannot be discretised with the standard approaches currently used in cloth simulation. We will therefore consider alternative ways. Since curvature is a central variable, we will briefly review some related concepts from differential geometry. The next section shows how a general transition to the discrete setting can be made. This work concludes with a discussion of the presented material and an outlook on how a physically accurate model for bending can be devised.

2 Bending

This section starts with an overview of bending models used in physically based simulation. Although the

Permission to make digital or hard copies of all or part of this work for personal or classroom use is granted without fee provided that copies are not made or distributed for profit or commercial advantage and that copies bear this notice and the full citation on the first page. To copy otherwise, or republish, to post on servers or to redistribute to lists, requires prior specific permission and/or a fee.
SHORT COMMUNICATIONS proceedings, Vol.9, No.1., ISBN 80-86943-05-4
WSCG 2006, January 30 - February 3, 2006, Plzen, Czech Republic.
Copyright UNION Agency – Science Press.

exact form depends on the actual method, the general steps to set up a physically based model for elastic deformations on a discrete representation of an object can be summarised as follows: first, an elastic energy E resulting from deformation has to be determined. This involves a material law relating strain to stress. In the case of bending energy, this strain is a change in curvature. By differentiation of E with respect to nodal positions, the force acting on a vertex is obtained. Lastly, if an implicit integration scheme is used for stepping forward the system over time, the Jacobian of the nodal forces has to be computed, too. Therefore, second order derivatives of all terms contributing to the energy have to be available. Since the computation of these derivatives can become very complex, some of the following methods model bending forces directly without relation to energy.

2.1 Existing Bending Models

In the seminal work of Terzopoulos et al. [TPBF87] a model for the animation of elastically deformable surfaces based on continuum mechanics is presented. The authors derive an elastic strain energy depending on nonlinear differential quantities, namely the metric and curvature tensors. The associated partial differential equations are discretised in space using finite differences on a regular quadrilateral grid. Although this approach is based on a physically sound theory, it was not widely adopted in the computer graphics community, due to its significant computational complexity. In the following years, approaches for the simulation of deformable surfaces like cloth mainly relied on particle and mass-spring systems. For modelling forces due to bending deformation, most of these methods use some kind of angular measure to approximate curvature. Breen et al. [BHW94] were among the first to use a coupled particle system in cloth simulation. The authors present an approach based on energy potentials for modelling the static drape of cloth. Departing from linear beam theory (see section 3), they first derive the bending energy between two successive edges in a rectangular discretisation. Curvature is approximated by fitting a circle through the three points involved. For large bending deformations, a different measure is used which in sum yields a biphasic curvature expression. Breen et al. model bending energy using data obtained from measurements with the *Kawabata Evaluation System* (KES) [Kaw80]. The corresponding nonlinear stress-strain curves are approximated numerically with quadratic fits. Once energies are set up at the nodes, the gradients have to be computed to obtain nodal forces. The approach presented by Eberhardt et al. [EWS96] extends this work to the dynamic range. Computation times are greatly reduced using sophisticated integration schemes. Eberhardt et al. do not explicitly approximate curvature but directly use the angle as a deformation measure.

Volino et al. [VCMT95] use a mass-spring system inspired by continuum mechanics. The basic bending element is formed by two adjacent triangles from the underlying unstructured grid. To determine curvature, a circle fitting inside the two triangles is found using the dihedral angle. The curvature over an element is then obtained as the inverse of the circle's radius. The authors point out that the curvature has to be limited to a certain maximum to prevent bending forces from growing to infinity. The actual forces are deduced from the geometry of the involved triangles using linear beam theory. Baraff et al. [BW98] use the same basic bending element as in [VCMT95]. Following their proposed computational framework, a constraint expression for bending energy is derived. This essentially corresponds to an energy term which depends quadratically on the dihedral angle.

A different approach to cloth simulation was proposed by Eischen et al [EDC96, EB00]. Their method is based on the nonlinear shell theory derived by Simo et al. [SFR89]. A four node bilinear element with nodal displacements and director rotations as the primary unknowns is used for discretisation (see [SFR89]). In the context of shell theory, curvature is directly accessible through bending strains and does not need not be approximated otherwise. Like in [BHW94] Eischen et al. use measured data obtained from the KES and approximate the curves with a 5th-order polynomial fit. In sum, the approach leads to highly nonlinear equilibrium equations which have to be solved, for example, with the Newton-Raphson procedure. This solver is coupled with an adaptive arc length control to account for limit or bifurcation points in the solution due to buckling instabilities. The proposed method is limited to the static case and does not account for dynamic effects. For subsequent comparison, Eischen et al. [EB00] present a particle-based approach based on principles found in continuum mechanics. Like Breen et al. they use a regular quadrilateral discretisation along with linear elasticity theory. However, they derive forces directly without explicit resort to energy potentials. Bending forces are computed using linear beam theory which again results in a linear moment-curvature relationship. The angle formed by two consecutive edges is taken as a direct measure for curvature. The authors state that the results of the two methods cannot be visually distinguished on the scale of the images they produced.

More recently, Choi et al. [CK02] proposed a bending model based on assumptions on the buckling behaviour of fabric. Departing from a quadrilateral mass-spring system, the basic bending element consists of an interleaved spring. The authors advocate that compressive in-plane forces on textiles lead to large out-of-plane deflections once a critical loading is reached. For the notoriously unstable post-buckling

state the buckled shape is predicted as a circular arc of constant length and curvature. With this assumption, the curvature can be computed analytically without angular expressions appearing. Hence, linear beam theory can be applied to derive the bending energy. Lastly, the authors derive expressions for force vectors and Jacobians at the nodes required in an implicit time integration scheme.

Bridson et al. [BMF03] proposed another derivation of bending forces for cloth animation. Again, two adjacent triangles form the basic bending element. With the requirement that bending forces should neither cause in-plane deformation of the fabric nor lead to rigid body motions, they derive the directions and relative magnitudes for the four bending force vectors of an element. These vectors are then scaled with a bending stiffness constant and the sine of the dihedral angle. An additional scaling factor accounts for anisotropy of the mesh. For the numerical time integration, Bridson et al. suggest to use a mixed implicit-explicit integration scheme in which the (comparably small) bending forces can be handled in an explicit manner while viscous damping forces are treated implictly. Thus, the computation of the complicated derivatives of the bending forces is avoided.

While most of the previous approaches use a rather rough curvature approximation, Grinspun et al. [GH$^+$03] presented a method which is based on a sound curvature derivation. Their work extends existing cloth simulators to the range of objects with a strong resistance to bending deformation. To this end, a discrete flexural energy potential is established using differential geometry (see section 5). Again, the basic bending element consists of two adjacent triangles. The energy derives from an approximation to the squared difference of mean curvature in the current and initial configuration. A drawback of this approach is that the derivatives of the bending energy are intricate to compute. Because of this complexity, the authors suggest the use of an automatic differentiation system.

Yet another way to treat bending was proposed by Etzmuß et al. [EKS03]. They use a discrete approximation of the surface Laplacian to model curvature. This has some aspects in common with the discrete mean curvature computation described in section 5. In the context of a linear finite element approach the Laplacian is computed for each element and projected onto the corresponding vertex normals. The element contributions are summed up to give the pointwise value for every vertex.

2.2 The Concept of Bending

Common deformation modes in 3D continuum mechanics are stretching and shearing. These modes are orthogonal to each other: pure stretching does not lead to shear deformation and *vice versa*. The pointwise view of (3D) continuum mechanics does not account for bending since it is indifferent of shape. The

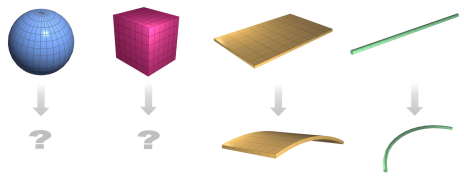

Figure 1: Whether an object can be bent depends mainly on its shape.

ability to bend an object is, however, closely related to its shape, or more precisely, to the proportion of its extents in the different dimensions. Consider e.g. a thin plate as shown in Figure 1. Here, one direction can be distinguished, in which the lengths are clearly inferior to those in the orthogonal directions. In this case, the intuitive bending deformation is such that it causes as little in-plane deformation as possible – a pure change in curvature. For a parametric surface which can be thought of as an infinitely thin plate this bending deformation can be determined analytically (see section 4). We examine the notion of bending for objects with finite thickness subsequently.

2.3 Bending with Finite Thickness

For a cylindrically bent plate (see Fig. 1), we can – without loss of generality – restrict our investigations to a thin slice. Thus, we arrive at a geometry corresponding to the classical beam element. A cross-sectional view of such a beam is shown in Figure 2. It can be seen that during deformation the bottom layer is stretched while the top layer is compressed (cf. [Kee99]). We can reasonably assume that the maximum values of tension and compression occur on the boundary layers. If we further assume that the induced stresses vary monotonically between these maxima we arrive at an axis with zero stress, the so called *neutral axis* (see Figure 2). These ge-

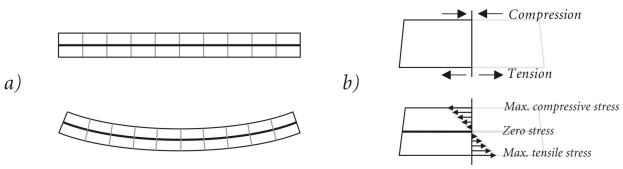

Figure 2: Beam geometry. *a)* Cross-sectional view of bending deformation. *b)* Linearly varying stresses through the thickness and *neutral axis*.

ometric relations motivate an analytic treatment of the problem in which the neutral axis is the primary parametrisation domain. This dimension reduction is the starting point for the theory of beams and plates which is introduced next.

3 Linear Elasticity of Beams and Plates

This section presents models for bending dominated problems known from engineering sciences. The simplest model corresponding to our interests is the 1D linear elastic beam. As we have seen in section 2, many existing approaches to bending in cloth simulation rely on this model. Because the stretching deformation of the neutral-axis is assumed to be negligible, the central unknown is the lateral deflection w of the neutral axis. The kinematic constraints leading to the common *Euler-Bernoulli* beam derive from the Kirchhoff-Love Assumptions: lines that are initially normal to the neutral axis remain straight, normal, and unstretched. The deformed state of the beam can be described by the displacements u_0 and w_0 of the neutral axis and a rotation θ of the normal (see Figure 3). The horizontal and vertical displace-

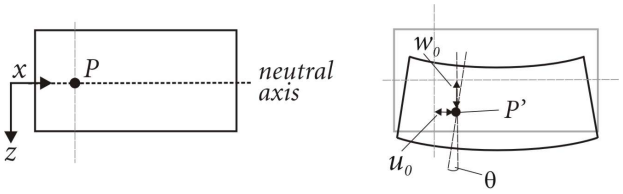

Figure 3: Displacements u_0 and w_0 of the neutral axis and cross-sectional rotation θ for a deformed beam element.

ments of any material point in the beam are given by $u(x,z) = u_0(x) - z\theta(x), \quad w(x,z) = w_0(x)$, and the generalised strain follows as $\varepsilon_x = \frac{\partial u}{\partial x} = \frac{\partial u_0}{\partial x} - z\frac{\partial \theta}{\partial x}$ (see [ZT00a]). Because normal lines are assumed to remain unstretched, the strain ε_z in this direction can be neglected. Using the second assumption, the transverse shear strain ε_{xz} equally vanishes.

With the strain defined, the stress now follows by the use of an appropriate constitutive law. For a linear elastic material law the stress is

$$\sigma_x = \frac{E}{1-\nu^2}\varepsilon_x \ , \tag{1}$$

where E is Young's modulus and ν is Poisson's ratio. The bending moment around the horizontal axis is obtained as

$$M = D\frac{\partial \theta}{\partial x} = \frac{Eh^3}{12(1-\nu^2)}\frac{\partial^2 w_0}{\partial x^2} \ . \tag{2}$$

Note the term $\frac{\partial^2 w_0}{\partial x^2}$ which, for small deflections w_0, is actually the curvature κ of the beam. Thus, equation (2) can be written in a clearer manner as $M = D\kappa$. This linear moment-curvature relationship is exploited by some approaches in cloth simulation to directly model bending forces (e.g. [VCMT95]).

The governing equations are established by considering the forces acting on a differential beam element (Fig. 4). The beam is in equilibrium if the transverse

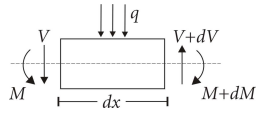

Figure 4: Distributed lateral forces q, transverse shear force V, and bending moment M acting on a differential beam element dx.

internal force V (or shear resultant) and the external distributed load q are in balance. Along with the moment equilibrium this leads to the equilibrium equation of the Euler-Bernoulli beam

$$\frac{Eh^3}{12(1-\nu^2)}\frac{\partial^4 w}{\partial x^4} = -q \ . \tag{3}$$

The above formulations directly carry over to cylindrically deformed plates. They can as well be translated to the general case of (doubly curved) thin plates (see [ZT00b]). In engineering, thin plate elements are used to support lateral loads. Because curvature now occurs in both transverse directions, one speaks of the *neutral surface*, or simply *mid-surface*, in analogy to the neutral plane. Again, it is assumed that the stretch deformations of the mid-surface are negligible. Hence, the primary unknown is again the lateral deflection w. However, the deflection now varies in both x and y direction which renders the problem two-dimensional. For thin plates, the governing equation turns out to be

$$\frac{Eh^3}{12(1-\nu^2)}\left(\frac{\partial^4 w}{\partial x^4} + 2\frac{\partial^4 w}{\partial x^2 \partial y^2} + \frac{\partial^4 w}{\partial y^4}\right) = -q \ . \tag{4}$$

This is a biharmonic equation involving fourth order partial derivatives. Investigating the corresponding strains it can be seen, that second order derivatives of the (lateral) displacement field are required. The thin plate equations have been used in computer graphics, too. For instance, they appear in a common minimisation problem from variational design (see e.g. [WW98]). Despite its demands on continuity, the thin plate approach can be used in physically based simulation. Since this theory does not take into account in-plane deformations it has to be augmented by an appropriate membrane model for this purpose. This conjunction can be found in the class of *Kirchhoff-Love* thin shell theories.

As already mentioned in the introduction, in most of the existing techniques for the simulation of thin flexible objects, the displacement basis required in thin plate analysis is not available. Nevertheless, many approaches make use of the Euler-Bernoulli beam equations to model bending, for example, directly along the edges of the underlying mesh. It is also possible to set up bending energies for the discrete setting, say, in terms of mean-curvature (see [GH$^+$03]). All of the methods that rely on such a physical model must necessarily use some kind of

curvature measure. Therefore, it is worth investigating what properties a reasonable curvature measure should have. To this end, we will proceed with some relevant material from differential geometry in the next section.

4 Curvature from Differential Geometry

The following concepts from differential geometry are mainly based on [Opr97] and [MDSB03]. The reader interested in a more detailed discussion is referred to the original work. Let $\mathcal{S}$ be a surface (2-manifold) embedded in 3D space with a parametric description

$$\mathbf{r}(\theta^1, \theta^2) = (x(\theta^1, \theta^2), y(\theta^1, \theta^2), z(\theta^1, \theta^2)) \ , \qquad (5)$$

where θ^1 and θ^2 are surface coordinates. At any point $\mathbf{p}$ on the surface, the two tangent base vectors are spanned by the partial derivatives of the mapping (5) with respect to the surface coordinates

$$\mathbf{a}_\alpha = \frac{\partial \mathbf{r}}{\partial \theta^\alpha} \ . \qquad (6)$$

The surface normal at this point is simply the cross-product. Curvature expressions for $\mathcal{S}$ at a point $\mathbf{p}$ are derived from lines on the surface defined as follows: for every direction $\hat{\mathbf{e}}_\varphi$ in the tangent plane let c_φ denote the curve that results from the intersection of $\mathcal{S}$ with the plane spanned by the surface normal $\mathbf{n}$ at $\mathbf{p}$ and $\hat{\mathbf{e}}_\varphi$ (see Figure 5).

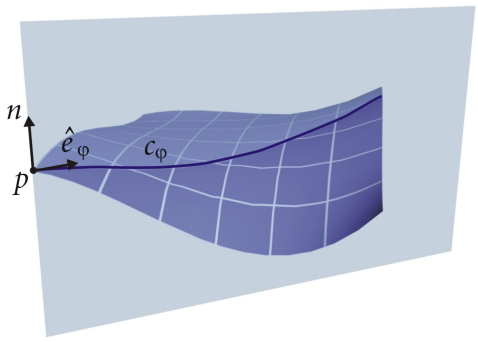

Figure 5: The surface curve c_φ is the intersection of the surface $\mathcal{S}$ with the plane spanned by the normal $\mathbf{n}$ and the unit direction vector $\hat{\mathbf{e}}_\varphi$.

The curvature of c_φ is called the *normal curvature* κ_N of $\mathcal{S}$ in the direction $\hat{\mathbf{e}}_\varphi$. The minimum and maximum of these values are called the *principal curvatures* κ_1 and κ_2. By integration over all unit directions the *mean curvature* at $\mathbf{p}$ is obtained as

$$\kappa_H = \frac{1}{2\pi} \int_{2\pi} \kappa_N(\varphi) d\varphi = \frac{\kappa_1 + \kappa_2}{2} \ , \qquad (7)$$

where the last equality follows from $\kappa_N(\varphi) = \kappa_1 \cos^2(\varphi) + \kappa_2 \sin^2(\varphi)$. A different expression for mean curvature is given by the *mean curvature normal*

$$\kappa_H \mathbf{n} = \lim_{diam(\mathcal{A}) \to 0} \frac{\nabla \mathcal{A}}{2\mathcal{A}} \ , \qquad (8)$$

where $\mathcal{A}$ is an infinitesimal area around a point and $diam(\mathcal{A})$ is its diameter (see [MDSB03]).

Another important local property of a surface is the *Gaussian curvature* κ_G which is defined as the product of principal curvatures $\kappa_G = \kappa_1 \cdot \kappa_2$. The Gaussian curvature is independent of the surrounding embedding of the surface: it measures only *intrinsic* curvature and is not affected by pure bending deformations as shown e.g. in Figure 1. Therefore, Gaussian curvature is not an appropriate measure for bending deformation. In contrast, normal and mean curvatures measure inextensional, extrinsic deformation and thus reflect changes due to pure bending. The following section gives an idea of how these quantities can be transferred to the discrete setting of triangle meshes.

5 Discrete Curvature

Almost every reasonable bending model used in the simulation of flexible materials incorporates some measure of curvature. Of course, every such model must necessarily result in a discrete formulation - whether it is derived from a partial differential equation or not. Hence, the interest in a discrete curvature measure is obvious. In the continuous case the curvature tensor provides a scalar value for every unit direction at every point of a surface. A discrete counterpart should give these data at distinct features (say vertices or edges) of the mesh as an average over the pointwise values of its attributed surface part. This value can then be plugged into the desired bending energy equation, from which forces are derived for every vertex in the (triangle) mesh in the usual way. Furthermore, it is desirable for computational aspects that the operator is easy to evaluate. It should have minimal support, i.e. only require information from a small local neighbourhood. Lastly, the operator should be independent of the actual discretisation of the surface. Of course, a central question is what kind of curvature should be measured? In the previous section we have seen that Gaussian curvature is inappropriate. For simple isotropic materials the mean curvature is sufficient and we will focus on this quantity. However, if anisotropic material behaviour is desired, the full curvature tensor will most likely be needed.

There has been abundant work on defining and computing discrete differential quantities, e.g. [PP93, Tau95a] and more recently [CSM03]. A concise and sound derivation of a complete set of discrete differential operators for triangulated 2-manifolds can be found in the work of Meyer et al. [MDSB03]. We take this work as a basis for the following overview.

5.1 The Laplacian and Derived Operators

Loosely spoken, curvature is related to second order derivatives. A commonly known differential operator based on second order derivatives is the *Laplace Operator* which in 2D Euclidean space is defined as

$$\Delta = \frac{\partial^2}{\partial x^2} + \frac{\partial^2}{\partial y^2} \ . \tag{9}$$

The discrete approximation of this operator on a regular quadrilateral grid can be expressed by the 5-point star

$$\mathbf{L}_1 = \begin{bmatrix} 0 & 1 & 0 \\ 1 & -4 & 1 \\ 0 & 1 & 0 \end{bmatrix} \ , \tag{10}$$

which is the result of taking second order finite differences in both dimensions. The generalisation of the Laplace operator from Euclidean space to 2-manifolds with Riemannian metric is called the *Laplace-Beltrami* operator. This is of interest here, because its discretisation leads to the mean curvature normal operator [Pol02a]. The question that arises is how this operator can be discretised on unstructured triangle meshes. Taubin [Tau95b] suggested to use an approximation which was later called the umbrella operator

$$\mathbf{L}_U = \frac{1}{m} \sum_{j \in N(i)} \mathbf{x}_j - \mathbf{x}_i \ , \tag{11}$$

where $N(i)$ is the set of neighbours of vertex i and m is the sum of the neighbour's valences. The advantage of this formulation is that it is linear in the vertex positions, just as the Laplacian on a regular quadrilateral setting. The drawback, however, is that it requires a specific parametrisation of the surface to be valid [KCVS98]. An extensions that accounts for irregularities is available but then the formulation is no longer linear [Fuj95]. As discussed subsequently, a more accurate approach is available in this case.

5.2 Discrete Differential Quantities

Generally, properties at a vertex of a mesh can be defined as spatial averages on the continuous surface around this vertex. Meyer et al. point out that with a consistent definition, the spatial averages will converge to the pointwise definition of the quantity in the limit. To this end, an appropriate area $\mathcal{A}$ has to be chosen, first. For a continuous function f defined on a surface $\mathcal{S}$, an average value f_{avg} over the area $\mathcal{A}$ can be obtained as

$$f_{avg} = \frac{1}{\mathcal{A}} \int_{\mathcal{A}} f \ du \ dv \ . \tag{12}$$

If such an average is to be assigned to every vertex of a triangle mesh $\mathcal{M}$ resulting from a discretisation of $\mathcal{S}$, an appropriate definition for the area $\mathcal{A}$ is important. It is desirable that the choice of $\mathcal{A}$ results in a (disjoint) partition of $\mathcal{M}$. Therefore, $\mathcal{A}$ must lie inside the 1-ring neighbourhood of $\mathbf{x}_i$ and the borders $\partial\mathcal{A}$ must cross the edges in their midpoints. It remains to choose which point the borders should pass through in the interior of a triangle. As two possibilities the barycenter or the circumcenter of the triangle can be chosen (cf. Figure 6). Selecting the circumcenter leads to a partitioning of $\mathcal{M}$ into *Voronoi* regions. Meyer et al. show that Voronoi regions are preferable

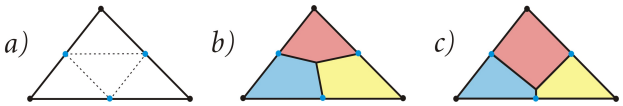

Figure 6: Alternative partitionings for a triangle. *a)* The border of any tiling must cross the mid-points of the edges. *b)* The barycenter is taken as interior point. *c)* Tesselation resulting from choosing the circumcenter as interior point.

over barycentric tilings, since they minimise the approximation error. Additionally, this partition is also useful for computing vertex masses needed for simulation (cf. [EKS03]). They derive a simple formula for the area $\mathcal{A}_V$ of the Voronoi region for vertex $\mathbf{x}_i$ as

$$\mathcal{A}_V = \frac{1}{8} \sum_{j \in N(i)} (\cot \alpha_{ij} + \cot \beta_{ij}) \left\| \mathbf{x}_i - \mathbf{x}_j \right\|^2 \ , \tag{13}$$

where α_{ij}, β_{ij} are the inscribed angles as shown in Figure 7. In case there is an obtuse triangle in the 1-ring neighbourhood, additional adjustments are necessary.

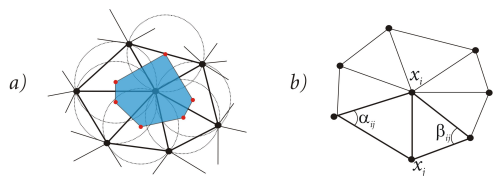

Figure 7: *a)* Voronoi region of a vertex. *b)* Angles for weighting edge $(\mathbf{x}_i - \mathbf{x}_j)$.

With an appropriate area for spatial averaging, the *mean curvature normal* operator $\mathbf{H}$ can be established. It is related to mean curvature as

$$\mathbf{H}(\mathbf{x}) = 2\kappa_H(\mathbf{x})\mathbf{n}(\mathbf{x}) \ . \tag{14}$$

Using the induced triangle metric, the mean curvature normal operator can be expressed as

$$\int_{\mathcal{A}} \mathbf{H}(\mathbf{x}) dA = -\int_{\mathcal{A}} \left(\frac{\partial^2 \mathbf{x}}{\partial u^2} + \frac{\partial^2 \mathbf{x}}{\partial v^2} \right) du \ dv \ , \tag{15}$$

where u and v describe a *conformal* (i.e. angle preserving) space parametrisation. With the definition of the Voronoi area (13) and additional transformations (see [MDSB03]), equation (15) turns into

$$\mathbf{H}_v(\mathbf{x}) = \frac{1}{2\mathcal{A}_V} \sum_{j \in N(i)} (\cot \alpha_{ij} + \cot \beta_{ij})(\mathbf{x}_i - \mathbf{x}_j) \ , \tag{16}$$

where the subscribt v signifies that the operator is vertex-related. This expression provides a simple and accurate way to determine mean curvature on triangular meshes. The operator requires only information from a small local neigbourhood and can be evaluated efficiently. Note, however, that it is nonlinear in terms of the involved vertex positions. As well as for vertices the mean curvature can also be defined on the edges of the mesh (see [Pol02b]). This may be more convenient for implementation issues.

6 Discussion

As we have seen there are quite a lot of approaches to modelling bending energy for the simulation of thin flexible objects. Most of them use only a rough curvature approximation mainly derived from angular deformations while others use a more sophisticated approach based on discrete curvature measures.

With the expressions from the previous section it is possible to set up approximate bending energies on discrete surface representations. These can then be used to compute force vectors and Jacobians at the vertices, needed in a simulation context. A related implementation was demonstrated in [GH$^+$03]. It must, however, be noticed that this model does not result from a discretisation of the thin plate (or shell) equations and is thus not as accurate as these methods known from engineering sciences. The corresponding energy expressions as well as first and second order derivatives are nonlinear in terms of the vertex positions. The computation of the derivatives bears additional complexity such that the overall costs will be higher than for standard approaches. Furthermore, using only mean curvature limits the application to isotropic materials. Computing the full curvature tensor would mean additional costs.

A question arising at this point is: what computational demands has an accurate approach based on physically more accurate models (e.g. the Kirchhoff-Love thin shell equations)? In order to reproduce the behaviour of thin flexible objects for a broad range of materials and independent of resolution, continuum mechanics are indispensable. Because of the shortcomings of finite difference schemes, the finite element approach will most likely be the method of choice for discretisation. Although these ingredients are commonly considered too costly for computer graphics, according to Hauth [Hau04] an efficient implementation leaves only a factor roughly between two and three when compared to standard approaches.

Basically, the thin plate equations impose certain smoothness requirements on the displacement field used in a finite element approach. More precisely, the displacement field has to be C^1-continuous. As a direct consequence the linear finite element approach presented by Etzmuß et al. cannot be simply extended to support the thin plate equations. The construction of an element type which provides a C^1-continuous displacement interpolation on its domain is not complicated. However, ensuring the continuity across elements is a major difficulty. Recently, a new paradigm for the finite element simulation of *thin shells* was introduced to the engineering community by Cirak et al. [COS00]. Using subdivision basis functions, they construct an element type with nodal displacements as only variables. The authors present a formulation of the thin shell equation which is linear in displacements. Hence, this is a promising way for the physically accurate modelling of bending in cloth simulation. In [TWS05] we therefore present an accurate and yet efficient approach to cloth simulation based on the work of Cirak et al.

ACKNOWLEDGEMENTS

Markus Wacker is supported by the Elitenförderung für Postdoktorandinnen und Postdoktoranden, Landesstiftung Baden-Württemberg. Bernhard Thomaszewski was supported by a grant from the Thomas-Gessmann-Stiftung.

References

[BHW94] D. Breen, D. House, and M. Wozny. Predicting the drape of woven cloth using interacting particles. In *SIGGRAPH proceedings '94*, pages 365–372. ACM Press, 1994.

[BMF03] R. Bridson, S. Marino, and R. Fedkiw. Simulation of clothing with folds and wrinkles. In *Proc. of ACM SIGGRAPH/Eurographics Symposium on Computer Animation (SCA 2003)*, pages 28–36. ACM Press, 2003.

[BW98] D. Baraff and A. Witkin. Large steps in cloth simulation. In *SIGGRAPH proceedings '98*, pages 43–54. ACM Press, 1998.

[CK02] K.-J. Choi and H.-S. Ko. Stable but responsive cloth. *ACM Transactions on Graphics (ACM SIGGRAPH 2002)*, 21(3):604–611, July 2002.

[COS00] F. Cirak, M. Ortiz, and P. Schröder. Subdivision surfaces: A new paradigm for thin-shell finite-element analysis. *International Journal for Numerical Methods in Engineering*, 47, 2000.

[CSM03] D. Cohen-Steiner and J.-M. Morvan. Restricted delaunay triangulations and normal cycle. In *Proc. of the 19th Annual ACM Symposium on Computational Geometry*, pages 237–246, 2003.

[EB00] J. Eischen and R. Bigliani. Continuum versus particle representations. In D. House and D. Breen, editors, *Cloth Modeling and Animation*, pages 79–122. A. K. Peters, 2000.

[EDC96] J. Eischen, S. Deng, and T. Clapp. Finite-element modeling and control of flexible fabric parts. *IEEE Computer Graphics and Applications*, 16(5):71–80, September 1996.

[EKS03] O. Etzmuß, M. Keckeisen, and W. Straßer. A Fast Finite Element Solution for Cloth Modelling. *Proc. of Pacific Graphics*, 2003.

[EWS96] B. Eberhardt, A. Weber, and W. Straßer. A fast, flexible, particle-system model for cloth draping. *IEEE Computer Graphics and Applications*, 16(5):52–59, September 1996.

[Fuj95] K. Fujiwara. Eigenvalues of laplacians on a closed riemannian manifold and its nets. In *Proc. of AMS*, pages 2585–2594, 1995.

[GH+03] E. Grinspun, , A. Hirani, M. Desbrun, and P. Schröder. Discrete shells. In *Proc. of ACM SIGGRAPH/Eurographics Symposium on Computer Animation (SCA 2003)*, pages 62–67. ACM Press, 2003.

[Hau04] M. Hauth. *Visual Simulation of Deformable Models*. Phd thesis, Wilhelm-Schickard-Institut für Informatik, University of Tübingen, Germany, July 2004.

[Kaw80] S. Kawabata. The standardization and analysis of hand evaluation. *The Textile Machinery Society of Japan*, 1980.

[KCVS98] L. Kobbelt, S. Campagna, J. Vorsatz, and H.-P. Seidel. Interactive multi-resolution modeling on arbitrary meshes. *SIGGRAPH '98 proceedings*, 20 April 1998.

[Kee99] S. Keeler. The science of forming: A look at bending. *Metal Forming Magazine*, pages 27–29, October 1999.

[MDSB03] M. Meyer, M. Desbrun, P. Schröder, and A. H. Barr. Discrete differential-geometry operators for triangulated 2-manifolds. In H.-C. Hege and K. Polthier, editors, *Visualization and Mathematics III*, pages 35–57. Springer-Verlag, Heidelberg, 2003.

[Opr97] J. Oprea. *Differential Geometry and its Applications*. Prentice-Hall, 1997.

[Pol02a] K. Polthier. Computational aspects of discrete minimal surfaces. *Proc. of the Clay Summer School on Global Theory of Minimal Surfaces*, 2002.

[Pol02b] K. Polthier. Polyhedral surfaces of constant mean curvature. *Habilitationsschrift TU Berlin*, 2002.

[PP93] U. Pinkall and K. Polthier. Computing discrete minimal surfaces and their conjugates. *Experimental Math.*, 2(1), 1993.

[SFR89] J. C. Simo, D. D. Fox, and M. S. Rifai. On a stress resultant geometrically exact shell model. part i: Formulation and optimal parametrization. In *Computational Methods in Applied Mechanics and Engineering*, volume 72, pages 267–302, 1989.

[Tau95a] G. Taubin. Estimating the tensor of curvature of a surface from a polyhedral approximation. *Proc. of ICCV*, pages 902 –907, 1995.

[Tau95b] G. Taubin. A signal processing approach to fair surface design. *Computer Graphics Proc.*, pages 351 – 358, 1995.

[TPBF87] D. Terzopoulos, J. Platt, A. Barr, and K. Fleischer. Elastically deformable models. In *SIGGRAPH proceedings '87)*, pages 205–214. ACM Press, July 1987.

[TWS05] B. Thomaszewski, M. Wacker, and W. Straßer. A consistent bending model for cloth simulation with corotational subdivision finite elements. Technical Report WSI-2005-19, Uni Tübingen, 2005.

[VCMT95] P. Volino, M. Courchesne, and N. Magnenat-Thalmann. Versatile and efficient techniques for simulating cloth and other deformable objects. In *SIGGRAPH proceedings '95*, pages 137–144. ACM Press, 1995.

[WW98] H. Weimer and J. Warren. Subdivision schemes for thin plate splines. *Computer Graphics Forum*, 17(3):303–314, 1998. ISSN 1067-7055.

[ZT00a] O. C. Zienkiewicz and R. L. Taylor. *The Finite Element Method. Volume 1: The Basis*. Butterworth Heinemann, 5th edition, 2000.

[ZT00b] O. C. Zienkiewicz and R. L. Taylor. *The Finite Element Method. Volume 2: Solid Mechanics*. Butterworth Heinemann, 5th edition, 2000.